Available online at www.sciencedirect.com
SCIENCE DIRECT
Journal of Catalysis 229 (2005) 12–23
JOURNAL OF CATALYSIS
www.elsevier.com/locate/jcat

Characterization and catalytic studies of PVD synthesized Mo/V/Nb/Te oxide catalysts

A.M. Gaffney [a], S. Chaturvedi [a], M.B. Clark Jr. [a], S. Han [a], D. Le [a], S.A. Rykov [b], J.G. Chen [b,*]

[a] *Rohm and Haas Company, Spring House, PA 19477, USA*
[b] *Center for Catalytic Science and Technology (CCST), Department of Chemical Engineering, University of Delaware, Newark, DE 19716, USA*

Received 19 May 2004; revised 2 September 2004; accepted 8 September 2004
Available online 12 November 2004

Abstract

Multicomponent Mo/V/Nb/Te oxide catalysts were synthesized using physical vapor deposition (PVD) onto the substrates of Si wafers and of honeycomb cordierites. The PVD films were prepared at different metal deposition sequences and were subsequently calcined at different temperatures and environment (air or N_2). The PVD films on Si wafer were characterized using several surface techniques, including X-ray photoelectron spectroscopy (XPS), near-edge X-ray absorption fine structure (NEXAFS), and secondary ion mass spectrometry (SIMS). In parallel, PVD films on cordierites were evaluated in a fixed-bed reactor for the selective oxidation of propane to acrylic acid. The combined synthesis, characterization, and reactor studies provided clear evidence that the surface compositions and the catalytic properties of the Mo/V/Nb/Te oxide catalysts depend strongly on the metal deposition sequence, calcination temperature, and calcination environment.

Keywords: Mo/V/Nb/Te oxides; PVD synthesis; XPS; NEXAFS; SIMS; Fixed-bed reactor; Selective oxidation; Propane; Acrylic acid

1. Introduction

The global abundance of low alkanes and the economic incentives of converting them to higher value petrochemicals or feedstocks have stimulated strong research interest in selective oxidation of alkanes [1,2]. Ammoxidation of lower alkanes, especially propane, is a process that has received much attention [3–6]. Fairly high yields of acrylonitrile from propane have been reported on a V–Sb–W–M–O-based catalyst [7] since the 1980s and on a Mo–V–Te–Nb–O catalyst [8] since the early 1990s. Research in the selective oxidation of propane to acrylic acid with molecular oxidation has been pursued world wide and a recent review of developments with mixed metal oxides has shown some promise [9].

The applications of multicomponent metal oxide (MMO)-type catalysts in propane oxidation to acrylic acid started in the 1990s, although Mo–V–Nb mixed oxides, the basis for these high performing propane selective oxidation catalysts, was initially developed in the 1970s for the oxidation of ethane to ethylene and acetic acid [10]. This Mo–V–Nb mixed oxide catalyst was also reported to be capable of activating propane at 300 °C but producing only acetic acid, acetaldehyde, and carbon oxides. To date, most of the applications of MMO-type catalysts are noted in patents [11–19]. All of these MMO catalysts are Mo based and most of them also contain V as a major component. Mo is the essential element of most commercial catalysts for propylene oxidation to acrolein and acrolein oxidation to acrylic acid while V is another essential element used as commercial catalyst for acrolein oxidation to acrylic acid.

The most effective catalysts to date for propane to acrylic acid are those Mo–V–Te–Nb–O catalysts reported by Ushikubo et al. [14]. A catalyst with the same four components was first found to be very effective for propane ammoxidation to acrylonitrile [20]. The performance of this Mo–V–Te–Nb–O catalyst for propane oxidation to acrylic acid has been shown to be significantly better than that of any other MMO type of catalysts [9]. Several reports have indi-

* Corresponding author.
E-mail address: jgchen@udel.edu (J.G. Chen).

0021-9517/$ – see front matter
doi:10.1016/j.jcat.2004.09.013

cated that both the composition of the catalyst and the preparation methods also greatly affect the catalyst performance, and that these performance differences of the catalysts reflect the structural differences of the catalysts prepared under various preparation conditions [18,21,22].

In this paper we describe a new catalyst synthesis method for preparing the Mo–V–Te–Nb–O catalysts by a physical vapor deposition (PVD) method. In essence, the corresponding metals were deposited onto silicon wafers and in various sequences, which were subsequently treated in air and or nitrogen to form mixed metal oxide compositions. The oxide materials were characterized using several surface science techniques. In addition, the corresponding metals were deposited onto cordierite honeycomb substrates in various sequences and then treated in air and/or nitrogen to form mixed metal oxides. These catalysts were evaluated in a fixed-bed reactor system for the conversion of propane to acrylic acid. This novel catalyst synthesis combined with reactor evaluation is the first one of its type for investigating the selective oxidation of propane to acrylic acid over PVD-synthesized catalysts.

2. Experimental

2.1. PVD synthesis

The mixed metal films of Mo–V–Nb–Te were deposited on either Si wafer or cordierite substrate by sequential physical vapor deposition, in a PVD system with a base pressure of 5×10^{-7} Torr. The metal sources were made by melting individual metal powders into different crucibles. The PVD system was equipped with four pockets that house four crucibles containing Te, Nb, V, and Mo, respectively. The advantage of having four metal sources at the same time is that the sequential deposition can be performed without opening the vacuum system to change metal sources. During deposition, an individual metal source was heated by electron beam, and the deposition rate (typically a few nanometers per minute) was monitored using a quartz crystal balance that was located near the honeycomb substrate. Three catalyst samples were synthesized on Si wafers using the following three sequences:

Sequence 1: Mo(72 nm)/V(19 nm)/Nb(10 nm)/Te(36 nm)/Si;
Sequence 2: Nb(10 nm)/ Te(36 nm)/Nb(10 nm)/V(19 nm)/Mo(72 nm)/Si;
Sequence 3: Te(36 nm)/Nb(10 nm)/V(19 nm)/Mo(72 nm)/Si.

As discussed later, the comparison of Samples 1 and 3 would determine the effect of deposition sequence, while the comparison of Samples 2 and 3 would reveal the effect of extra surface Nb. Only sequences 1 and 3 were utilized for the PVD deposition on the cordierite substrate.

The PVD films on Si wafers and on cordierite were subsequently oxidized using standard calcination procedures. The PVD samples were each calcined in a quartz tube. Each quartz tube was placed in an oven, at ambient temperature, with a 100 cc/min flow of air through the tube, the furnace was then heated from ambient temperature to 275 °C at 10 °C/min and held there for 1 h; then, using a 100 cc/min flow of either air or N_2 through the tube, the oven was heated from 275 to 600 °C at 2 °C/min and held there for 2 h.

The PVD films on Si wafers were calcined under various conditions. For example, the samples were held for 2 h at 600 and 675 °C to determine the effect of annealing temperature. In additions, samples were also held at 600 °C for 2 h in air or in N_2 to reveal the effect of annealing environment. All samples were calcined initially in air at 275 °C unless otherwise noted.

2.2. Spectroscopic characterization

The XPS experiments were performed on a KRATOS-Ultra instrument using a hemispherical energy analyzer. Monochromatic Al$K\alpha$ X-rays ($h\nu = 1486$ eV) were used as the excitation source. The source was operated at 300 W, 15 kV, 20 mA. All spectra were acquired at normal incidence, takeoff angle set at 90°, with the charge neutralizer switched on. The base pressure of the instrument was maintained at less than 5.0×10^{-10} Torr. The operating pressure for these films was 1.0×10^{-9} Torr. All survey scans were collected with a pass energy of 160 eV and a step size of 0.5 eV/step while the high-resolution spectra were collected with a pass energy of 20 eV and a step size of 0.05 eV/step. All binding energies were referenced to the carbon 1s CH_x component set to 284.6 eV.

The NEXAFS measurements were performed at the U1A Beamline at the National Synchrotron Light Source (NSLS) at Brookhaven National Laboratory. The NEXAFS spectra were recorded by means of electron yield, using a channeltron electron multiplier located near the sample. The NEXAFS spectra were recorded for O K edge and V L edge in the energy range of 500–590 eV; a grid containing Cr (L_{III}-edge energy at 576.5 eV) was placed in the beam path to calibrate the energy of the incident beam in this energy range.

The SIMS profiles were collected with an ion-ToF SIMS IV dual-beam time-of-flight secondary ion mass spectrometer. SIMS sputter depth profiles were obtained by cycling between a $^{69}Ga^+$ analysis mode and the high-current Ar^+ sputter mode. The sputter mode employed 3 kV $^{40}Ar^+$ (50 nA) focused into a 50-μm spot. The sputter gun was rastered over a 200 × 200-μm area. The analysis mode employed 15 kV $^{69}Ga^+$ (1.5 pA target current) primary ions pulsed at less than 1 ns. These experimental conditions provided mass resolutions of greater than 6000 at $m/z = 29$. The analysis area 20 × 20-μm analysis area was aligned in the center of the sputtered area. An O_2 jet was used with a partial pressure of 1×10^{-6} Torr. Secondary ion images were obtained by ras-

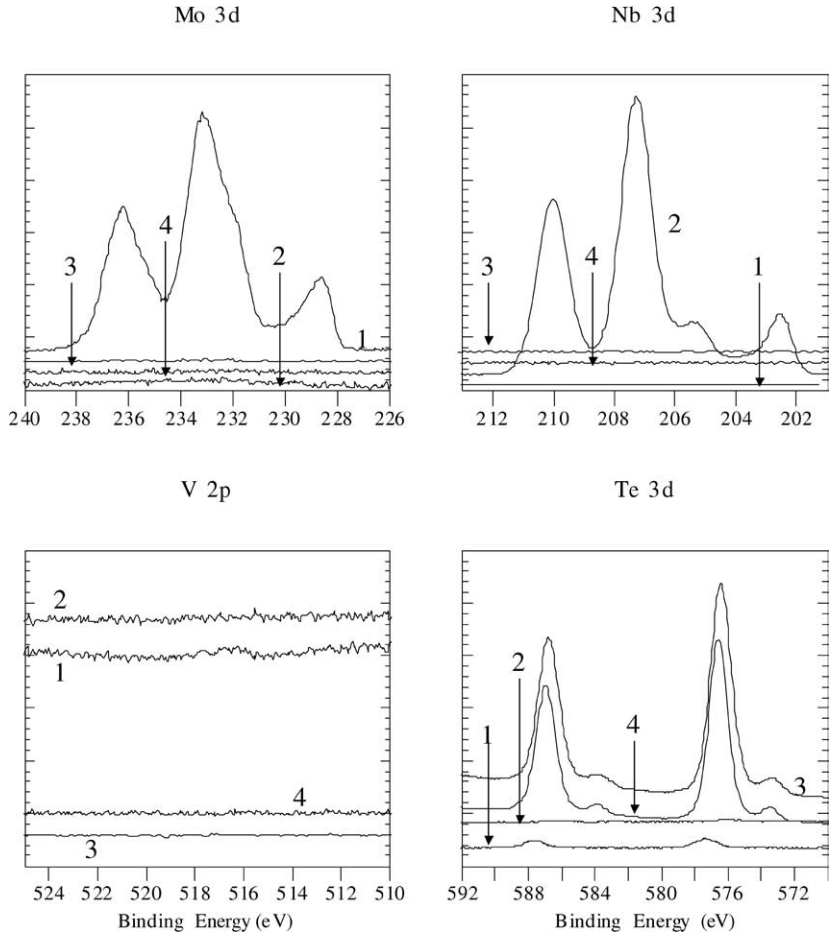

Fig. 1. XPS spectra of as-deposited films on Si wafers. Sample 1, Mo/V/Nb/Te/Si; Sample 2, Nb/Te/Nb/V/Mo/Si; Sample 3, Te/Nb/V/Mo/Si; and Sample 4, Te/V/Mo/Si.

tering the 15 kV $^{69}Ga^{+}$ primary ions over a 500 × 500-μm area using 128 × 128 pixels.

2.3. Catalytic evaluation

The PVD-coated cordierite substrates were evaluated in an Autoclave Engineer's Bench Top Reactor System to assess their activity toward the conversion of propane to acrylic acid. Evaluations were conducted in the fixed-bed, tubular reactor at 1 atm by passing a feed of 7% propane, 22% water, and balance air over the PVD-coated cordierite substrates inserted into the $\frac{1}{2}$ inch, quartz tubular reactor at temperatures ranging from 480 to 560 °C with a volumetric contact time of 3 s.

3. Results and discussion

3.1. XPS results

3.1.1. As-deposited films

Fig. 1 shows the Mo 3d, Nb 3d, V 2p, and the Te 3d XPS spectra for the as-received wafers. The sample numbers correspond to the following deposition sequences:

Sample 1: Mo/V/Nb/Te/Si;
Sample 2: Nb/Te/Nb/V/Mo/Si;
Sample 3: Te/Nb/V/Mo/Si;
Sample 4: Te/V/Mo/Si.

Examination of the top left panel in Fig. 1 shows Mo on the surface of the Mo-capped film (sample 1). The Mo 3d lineshape indicates the presence of Mo (metallic to +4 oxidation state at Mo $3d_{5/2}$ binding energy ∼ 228.4 eV), Mo in +5 oxidation state (Mo $3d_{5/2}$ binding energy ∼ 231.5 eV), and Mo in +6 oxidation state (Mo $3d_{5/2}$ binding energy ∼ 232.6 eV). The bottom left panel spectra show the absence of V 2p features which is consistent with the fact that there is no V-capped thin film. Shown in the top right panel are the Nb 3d spectra for the four films. It is evident that Nb is present only in the Nb-capped film with Nb $3d_{5/2}$ peaks centered at approx 202.4 eV (metallic), 205.1 eV (oxidation states between +2 and +4), and approx 207 eV (+5 oxidation state). The bottom right panel of Fig. 1 shows the Te 3d spectra for the four films. It can be seen that Te is present in all the four films, although it is at very low concentrations in the Nb or the Mo-capped film (see Table 1). For the Te-capped films (samples 3 and 4), the Te $3d_{5/2}$ bind-

ing energy of ∼ 576 eV indicates an oxidation state of +4. In addition the shoulder at 573 eV corresponds to the presence of metallic Te. The Nb-capped film (sample 2) contains a tiny amount of Te in +4 oxidation state (not seen in the spectra due to scale; see Table 1), whereas the Mo-capped film shows the Te $3d_{5/2}$ centered at approx 577 eV which corresponds to Te in +6 oxidation state. All these results taken together suggest that the "as-deposited" films do not have complete mixing of the metals and the capping layer exists in mixed oxidation states. The XPS compositions of the as-deposited films are presented in relative molar ratios in Table 1.

Table 1
XPS composition in relative molar ratios for the as-deposited films

Element	Mo/V/Nb/Te/Si Sample 1	Nb/Te/Nb/V/Mo/Si Sample 2	Te/Nb/V/Mo/Si Sample 3	Te/V/Mo/Si Sample 4
V	0.00	0.00	0.00	0.00
O	3.10	2.38	1.80	1.90
Mo	1.00	0.00	0.00	0.00
Nb	0.00	1.00	0.00	0.00
Te	0.07	0.02	1.00	1.00
Si	0.29	0.00	0.00	0.03

Interestingly, if we were to assume that all oxygen detected via XPS is associated with the capping metal layer, then the surface compositions indicate that the Mo-capped film is mainly MoO_3, Nb-capped film is mostly Nb_2O_5, and the Te-capped films are mainly TeO_2.

3.1.2. Air versus nitrogen calcination

The effect of the calcination environment was investigated using XPS. Shown in Fig. 2 are the XPS spectra for sample 2 (Nb/Te/Nb/V/Mo/Si deposition sequence) calcined under various conditions. The samples numbers correspond the following calcinations conditions:

Sample 2: Nb/Te/Nb/V/Mo/Si deposition sequence;
Sample 2A: Sample 2 calcined in air at 600 °C;
Sample 2B: Sample 2 calcined in N_2 at 600 °C;
Sample 2C: Sample 2 calcined in air at 675 °C.

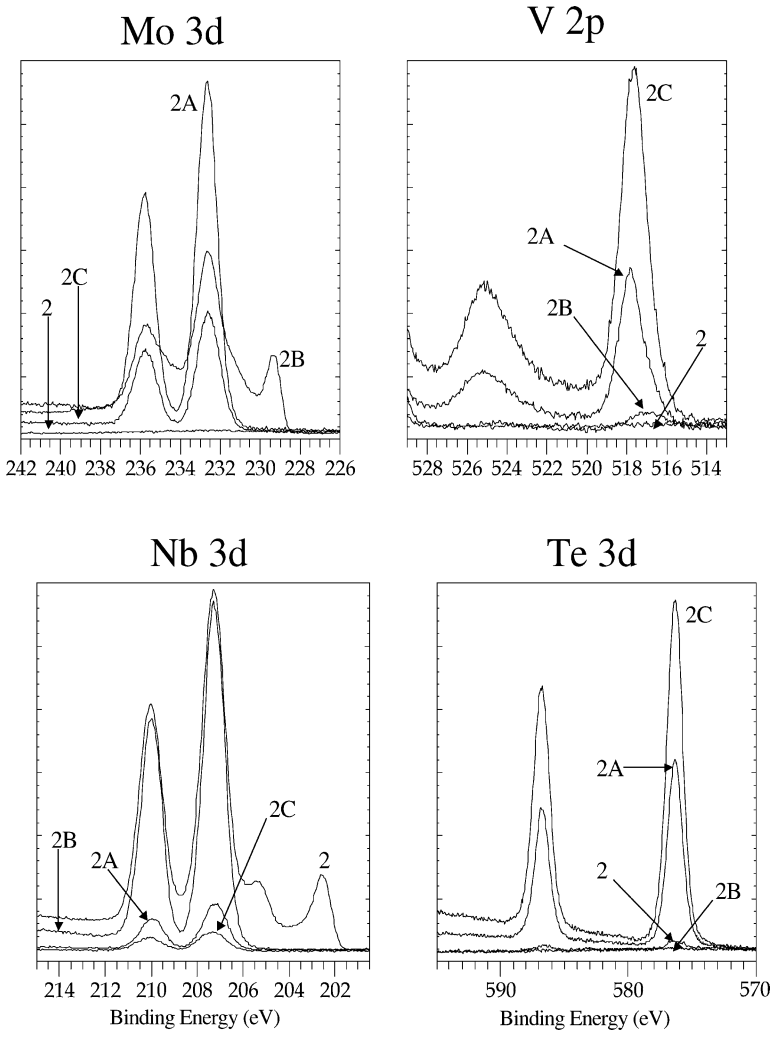

Fig. 2. XPS spectra of sample 2 (Nb/Te/Nb/V/Mo/Si) calcined under various conditions. Sample 2A, calcined in air at 600 °C; Sample 2B, calcined in N_2 at 600 °C; Sample 2C calcined in air at 675 °C.

Table 2
Standard heats of formation of relevant oxides

Compound	Standard heat of formation ΔH_f° (kJ/mol)
MoO_2	−588.9
MoO_3	−745.1
TeO_2	−322.6
NbO	−405.8
NbO_2	−796.2
Nb_2O_5	−1899.5
VO	−431.8
V_2O_3	−1218.8
V_2O_5	−1550.6
SiO_2	−910.7

Table 3
XPS composition in relative molar ratios for wafer 2 (deposition sequence = Nb/Te/Nb/V/Mo/Si) calcined under various conditions

Element	Bulk target composition	Sample 2A 600 °C, 2 h/air	Sample 2B 600 °C, 2 h/N_2	Sample 2C 675 °C, 2 h/air
V	0.3	0.50	0.05	1.68
O		6.39	3.99	13.61
Mo	1.0	1.00	1.00	1.00
Nb	0.12	0.20	0.72	0.31
Te	0.23	0.46	0.01	1.61
Si		0.767	0.00	1.67

The top right panel of the Fig. 2 shows that calcination in air drives V to the surface of the film. The V $2p_{3/2}$ peak centered at a binding energy of approx 517.5 eV corresponds to highly oxidized V. From a thermodynamic perspective, it possible that the formation of V_2O_5 is the driving force for the surface segregation of V. Standard heats of formation for the relevant oxides are given in Table 2. The highest heat of formation for Nb_2O_5 may explain why the Nb in all films is present in a +5 oxidation state.

The top left panel in Fig. 2 displays the Mo 3d spectra for the air- and nitrogen-calcined films and it can be seen that the films which are calcined in air (samples 2A and 2C) show a single Mo 3d doublet with the Mo $3d_{5/2}$ centered at 232.6 eV which corresponds to Mo +6 (probably MoO_3). On the other hand, the film that was calcined in nitrogen shows reduced oxidation states of Mo, in addition to Mo +6. The nitrogen-calcined samples were exposed to air during sample transfer to the XPS chamber. The detection of reduced Mo on these samples suggested that the exposure to air did not lead to the complete oxidation of the surface Mo to Mo +6. The presence of partially reduced Mo states may be an important step in propane activation since a partially reduced state presents a coordinatively unsaturated site for the propane molecule to attach itself. If all the Mo is completely oxidized, it is coordinatively saturated and the propane molecule has nowhere to attach. This is why we believe that calcination in N_2 is an important step for obtaining a catalyst with the desirable distribution of oxidation states. Calcination in air results in complete oxidation of the catalyst, which is detrimental to its catalytic activity as discussed later.

Note that among all the relevant oxides, TeO_2 has the lowest heat of formation (−322 kJ/mol). The Te 3d spectra indicate that Te segregates to the surface for the air-calcined film but not for the nitrogen-calcined film. In other words, there is not enough of a thermodynamic force for the formation of tellurium oxides at low temperatures since all samples were calcined in air at 275 °C. Higher temperature (600 °C) would also offer a kinetic advantage for Te diffusion.

The XPS compositions of samples 2A, 2B, and 2C are presented in relative molar ratios in Table 3. Note that all compositions have been normalized to Mo = 1.00. The composition of the as-deposited film did not show any evidence for the presence of Mo on the surface. Both these results taken together indicate that there is good mixing of Mo upon annealing (regardless of the calcination environment). We have conducted ESCA depth profiles (not shown) which indicate good homogeneous mixing of all elements present in the calcined thin films. It is interesting to note that despite the good mixing, the XPS composition of the samples is not even close to the targeted bulk composition.

Another noteworthy point is that the oxygen content in the air-calcined film is considerably higher than in the nitrogen-calcined film. This is presumably because all metals are in their highest oxidation states in the air-calcined films. Based on the standard heats of formation alone, one would expect higher Nb levels than Te levels on the surface of the film. However, this is not the case here. One reasonable explanation could be that the formation of Nb oxide while thermodynamically favorable is a kinetically limited process whereas, formation of Te oxide is thermodynamically not such a favorable process but is kinetically favored.

3.1.3. 600 °C versus 675 °C calcination

The effect of the calcination temperature was investigated using XPS. Shown in Fig. 2 are the XPS spectra for wafer 2 (Nb/Te/Nb/V/Mo/Si deposition sequence) calcined in air at 600 °C for 2 h. Also shown are the corresponding spectra for the same wafer calcined in air at 675 °C for 2 h. The top right panel of Fig. 2 shows that both films have the V $2p_{3/2}$ peaks centered at a binding energy of approx 517.5 eV, which corresponds to highly oxidized V. The Mo 3d spectra show a single doublet for both films that corresponds to Mo in +6 oxidation state. The Nb 3d spectra are also similar in that Nb is oxidized as +5. The Te 3d spectra are also similar and indicate the presence of Te between +4 and +6 oxidation states. There are, however, differences in the relative metal ratios (see Table 3).

Note that the higher temperature calcinations result in higher V, Nb, and Te concentrations on the surface of the film. This is consistent with our earlier hypothesis that formation of Nb oxide is a kinetically limited process and also that the formation of Te oxide is kinetically favored. Another noteworthy point is that the oxygen content is higher in the film that is calcined at a higher temperature. All these data suggest better mixing of the films at 675 than at 600 °C.

If you assume complete oxidation of the metals when the calcinations is done in air, i.e., Mo → MoO_3, Nb → Nb_2O_5, V → V_2O_5 and Te → TeO_3, then using the metal ratios given in Table 3, one would expect that the oxygen content should be 6.1 (for the air-calcined film at 600 °C), which is only slightly less than the experimentally measured value of 6.4. The calculated oxygen value for the air-calcined film at 675 °C is 12.8, which is again only slightly less than the experimentally observed value of 13.6. This discrepancy may be accounted for by considering that some oxygen is also going to be associated with the Si atoms.

Overall, the XPS results presented in Figs. 1 and 2 and Tables 1–3 provide the following main observations: (1) The composition of the as-deposited film depends on the deposition sequence. (2) Calcination of the films in air or nitrogen results in the presence of all four elements on the surface. (3) Calcination in air results in complete oxidation whereas calcination in nitrogen results in the formation of reduced Mo species in addition to Mo (+6).

The XPS results clearly indicate that the surface compositions of the PVD samples depend on the calcination temperature (600 vs 675 °C) and environment (air vs N_2). The detection of different surface compositions, instead of an identical surface composition if thermodynamic equilibrium is achieved, suggests that the mixing of surface oxides is "kinetically controlled" in the current study. More detailed kinetic studies, such as calcination as a function of time or using cycles of N_2/air treatment, will be necessary to determine the role of kinetics and thermodynamics in the surface compositions of the calcined PVD samples.

3.2. NEXAFS results

NEXAFS is utilized to further characterize the compositional and electronic properties of the PVD films. As summarized in a recent review [23], NEXAFS spectrum at the O *K* edge is related to the dipole transition of O 1s electrons into the partially occupied and unoccupied orbitals. As a result the O *K*-edge spectrum is very sensitive to the local bonding environment of metal oxides. For example, Fig. 3 compares the O *K*-edge spectra of four metal oxides that are relevant to the current study, V_2O_5, MoO_3, Nb_2O_5, and TeO_2. The comparison clearly indicates that each oxide is characterized by a distinct set of O *K*-edge features. In addition, two additional features are present in the spectrum of V_2O_5, which are related to the V *L*-edge features [24]. The positions of these two features can be used to determine the oxidation state of V [24,25].

3.2.1. Effect of deposition sequence

Fig. 4 compares the NEXAFS spectra of PVD films from the three deposition sequences. All samples were calcined for 2 h at 600 °C in air prior to the NEXAFS measurements. In general the NEXAFS results support the conclusions from the XPS measurements. For example, based on the intensities of the two V *L*-edge features at 519.75 and 525 eV,

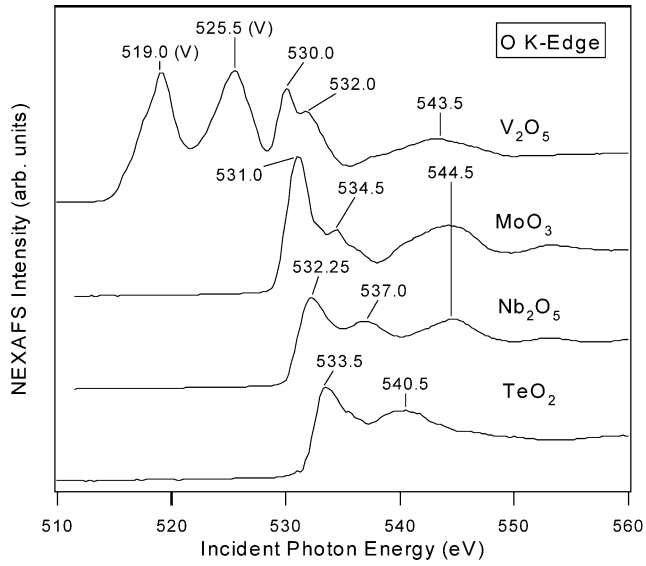

Fig. 3. Comparison of O *K*-edge spectra of four metal oxides that are relevant to the current study, V_2O_5, MoO_3, Nb_2O_5, and TeO_2.

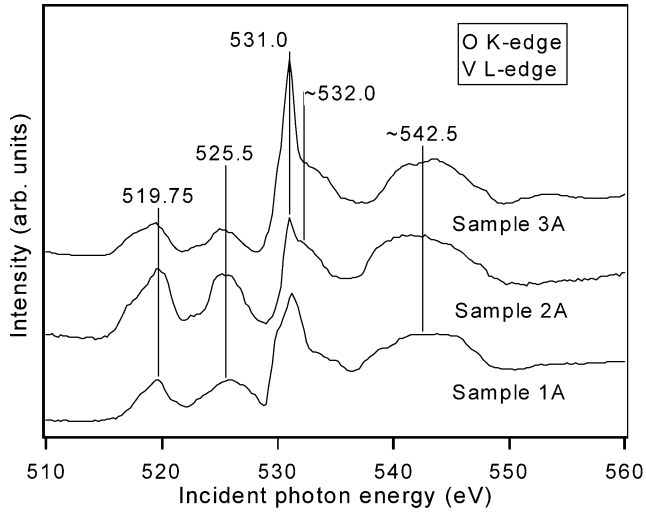

Fig. 4. Comparison of O *K*-edge and V *L*-edge spectra of PVD films prepared by different deposition sequences. The samples were calcined for 2 h at 600 °C in air.

the deposition sequence of Nb/Te/Nb/V/Mo/Si produces the highest surface vanadium oxide concentrations among the three samples. In addition, the energy positions of these two peaks are characteristic of V in the 5+ state. Furthermore, the detection of O *K*-edge features at 531.0 eV (characteristic of Mo–O bonds) and at ∼ 532 eV (characteristic of V–O bonds) indicates that both Mo oxides and V oxides are present near the surface region.

3.2.2. Effect of calcination temperature and environment

Fig. 5 compares the O *K*-edge and V *L*-edge features of PVD films, prepared using the deposition sequence of Nb/Te/Nb/V/Mo/Si, after being treated under different calcination conditions. Based on the intensities of the V *L*-edge features, calcination in air at 600 °C enhances the surface

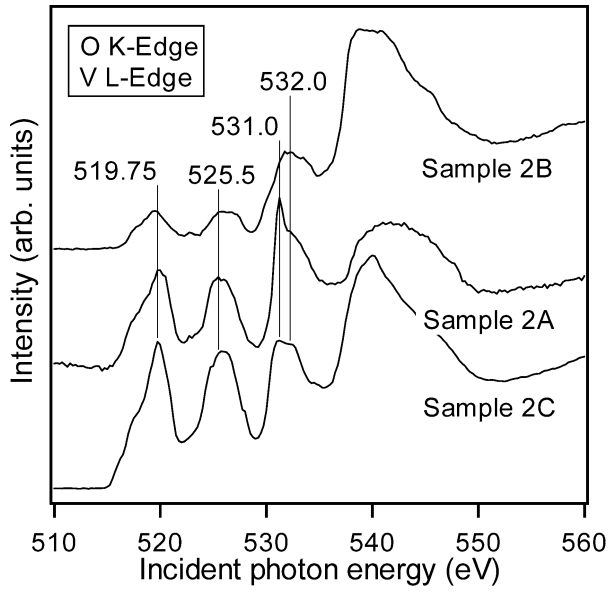

Fig. 5. Comparison of O *K*-edge and V *L*-edge spectra of Nb/Te/Nb/V/Mo/Si films after calcination for 2 h under different conditions. Sample 2A, 600 °C in air; Sample 2B, 600 °C in N_2; Sample 2C, 675 °C in air.

concentration of V oxides as compared to calcinations in N_2. In addition, the observation of a relatively more intense O *K*-edge feature at 531.0 eV indicates that calcination in air at 600 °C also enhances the surface concentration of Mo oxides. Both observations are consistent with the XPS measurements. The comparison in Fig. 3 also indicates that calcination in air at 675 °C further enhances the surface concentration of V oxides. Furthermore, the energy positions of the V *L*-edge features remain relatively constant after calcination in air and in N_2, suggesting that V is in the 5+ state in either calcination environment.

3.3. SIMS results and discussion

3.3.1. SIMS assessment of as-deposited films

SIMS profiles were collected from the four as-deposited films to check their integrity before the different annealing steps were performed. There is an inference between the major Te isotopes and MoO_2 ions. Therefore, we were forced to use ^{122}Te at 2.5% abundance to monitor Te location and concentration. Fig. 6 contains the SIMS profiles obtained from the four as-deposited films. The profiles obtained from all of the films, except the Mo/V/Nb/Te/Si, are consistent with the deposition. The profile from the Mo/V/Nb/Te/Si film suggests this film is Mo/V/Si with multiple layers that are enriched in Nb with Te concentrated in the Mo layer. As discussed below, we believe molybdenum appears to be an effective barrier layer. Without this barrier layer, there is a strong vanadium–silicon interaction.

3.3.2. Mixing as function of annealing temperature and atmosphere

The degree of mixing as a function of annealing temperature and atmosphere was accessed through SIMS profiling. Fig. 7 displays the SIMS profiles obtained from the Nb/Te/Nb/V/Mo/Si film as deposited and after annealing at 600 °C in air and nitrogen, and at 675 °C in air. All films were annealed for 2 h. The five original metal films are clearly evident in the as-deposited film. Annealing for 2 h in nitrogen results in incomplete intermixing. The niobium layers have interdiffused and enrich the air interface with distinct vanadium and molybdenum layers still present. Intermixing of the layers is obtained with 2 h of air calcinations at 600 °C. The intermixing appears to result in a film with different elemental concentrations as a function of depth. There is a slight enrichment of tellurium and vanadium at the air interface and the vanadium is again enriched near the silicon substrate. Silicon is also found to migrate through the film. Calcining the film at 675 °C in air for 2 h results in an enrichment of vanadium at the air interface and increased diffusion of silicon within the film.

3.3.3. Degree of mixing after annealing at 600 °C in air

SIMS profiles (shown in Fig. 8) were collected from the remaining films after being calcined at 600 °C for 2 h in air to ensure that the films were completely intermixed. The Mo/V/Nb/Te/Si film appears to be mixed; however, evidence of Te enrichment at the air interface and vanadium at the Si interface was detected. The Te enrichment at the air interface is limited to the first few nanometers of the film while the V-enriched layer extends over half the film. The Te/V/Mo/Si film displays similar behavior with a spike in the Te concentration at the air interface and a vanadium-enriched layer at the Si interface or "interphase." This V-rich layer is present in the bottom third of the film. The V/Mo intensity ratio is greater at the Si interface for the Te/V/Mo film than the Mo/V/Nb/Te film.

3.3.4. Air interface distributions as function of calcination treatment

The lateral distributions of Si, V, Nb, Mo, and Te at the air interfaces of the four Nb/Te/Nb/V/Mo/Si films discussed above were determined by SIMS imaging (shown in Fig. 9). The Si, V, Nb, Mo, Te, and total secondary ion images obtained from the as-deposited, and the 2 h annealed films at 600 °C in air, 600 °C in nitrogen, and 675 °C in air are compared in Fig. 9. The surface characterization of the as-deposited film agrees well with the XPS results, revealing an air interface that is composed of Nb. All four metals are detected at the air interface of the calcined films. In addition to the metals, Si is also detected at the air interface upon calcinations. The 600 °C air-calcined film reveals Si-enriched domains in dimensions of a few to 100 μm. The 600 °C nitrogen-calcined film appears to be "dewetting" with areas as large as 250 μm being exposed. The Si image obtained from the 675 °C in the air-calcined film suggests that the Si is present at vanadium-rich grain boundaries. Based on the degree of mixing and the surface characterization, the remaining films were calcined at 600 °C in air for 2 h.

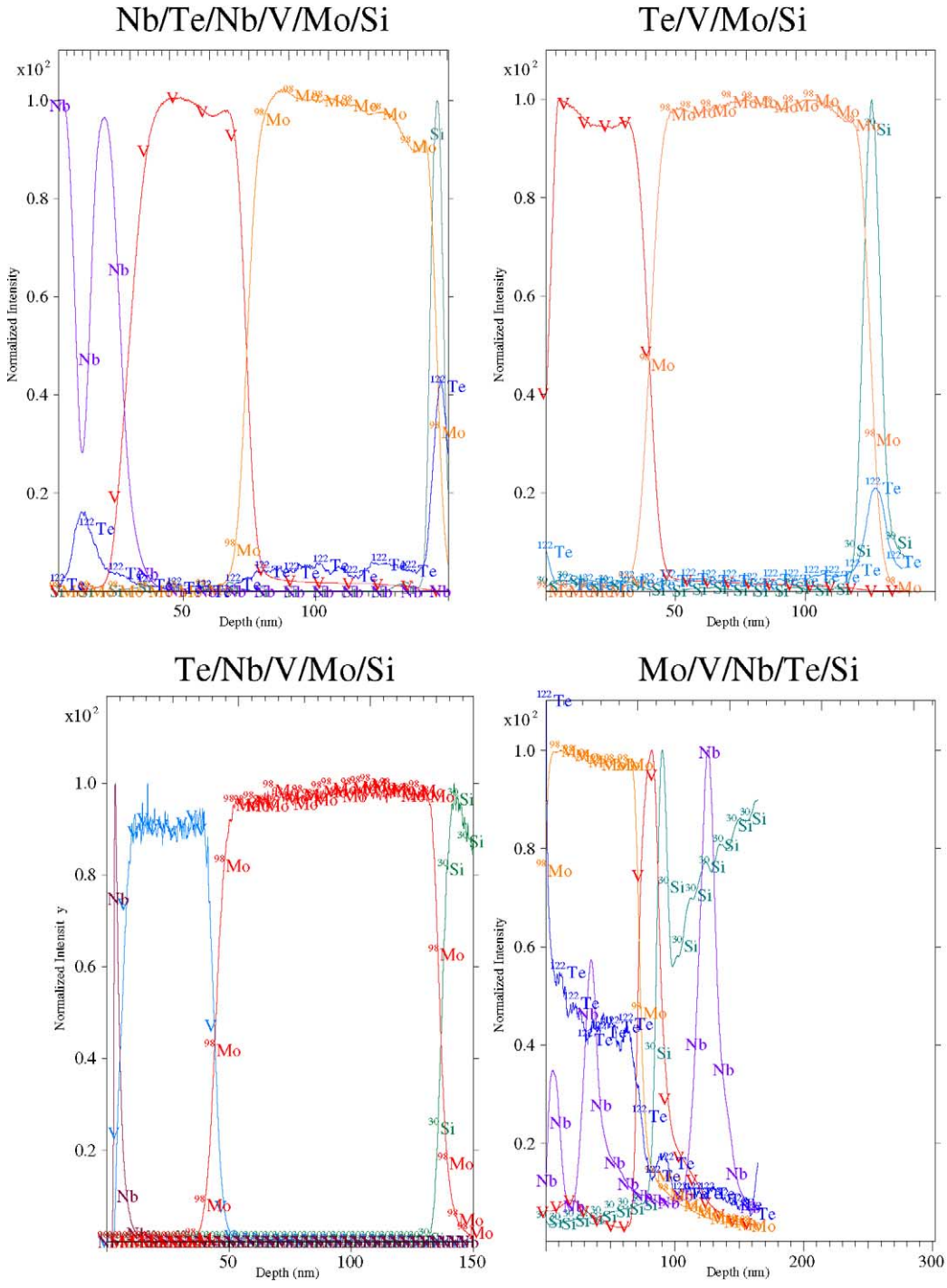

Fig. 6. SIMS profiles of as-deposited PVD films on Si wafers.

In summary, SIMS profiles were used to determine the degree of intermixing as a function of annealing temperature and atmosphere. When annealed in air for 2 h, 600 °C is sufficient to obtain intermixed films. When annealed in nitrogen for 2 h at 600 °C, some mixing has occurred; however, Nb-, V-, and Mo-enriched layers still exist. Secondary ion images reveal that Si is present at the air interface. Its location appears to be a function of annealing temperature and atmosphere. When annealed in air at 600 °C the Si appears to be located in Si-rich domains while annealing at 675 °C in air results in Si being located at grain boundaries. When annealed at 600 °C in nitrogen the films appear to "dewet."

3.4. Reactor evaluation

As described previously, the two PVD samples were prepared by deposition of the following metals in the sequences given below onto the cordierite substrate:

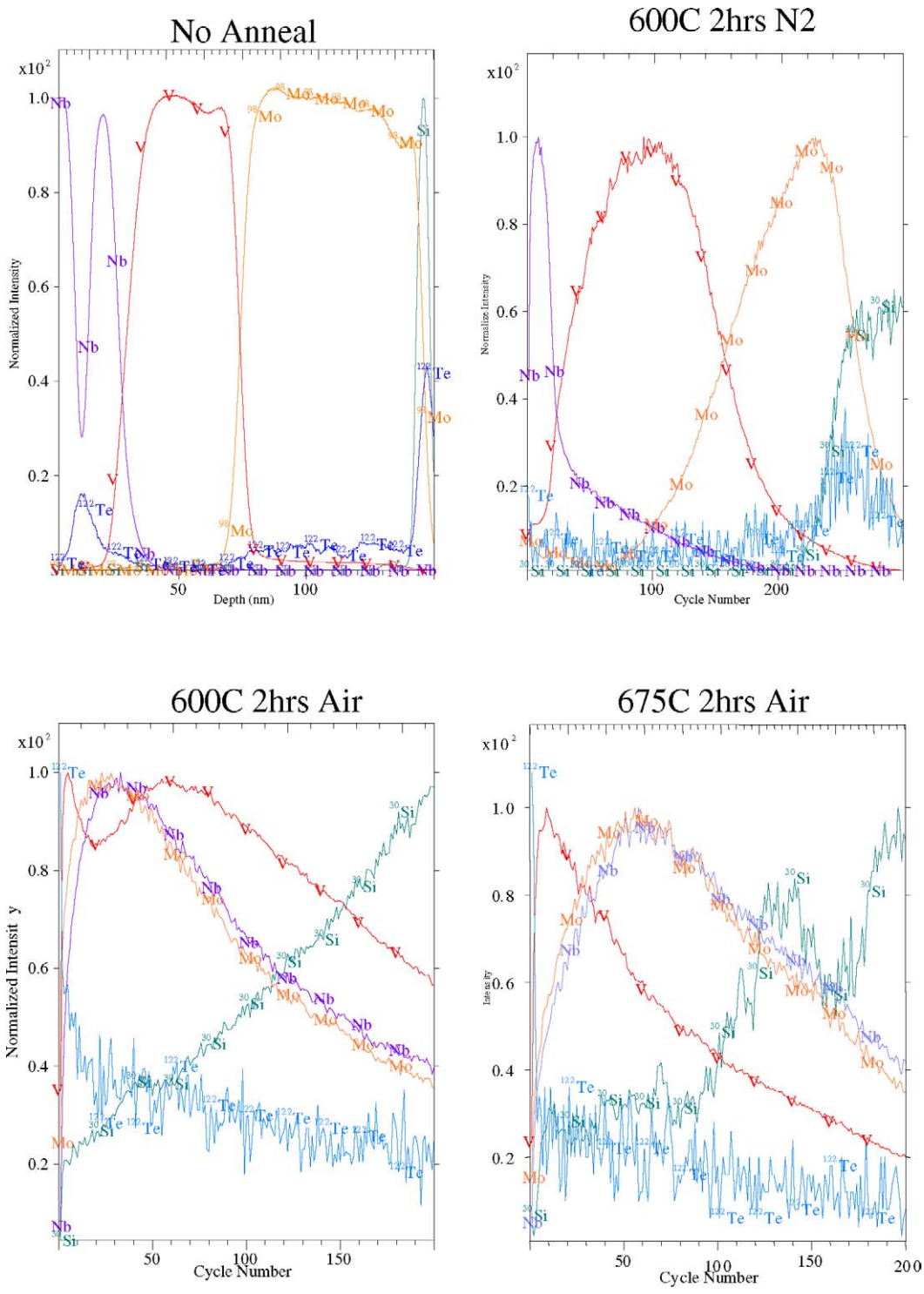

Fig. 7. SIMS profiles after calcination treatment of Nb/Te/Nb/V/Mo/Si films under different conditions.

Sequence 1: Mo(72 nm)/V(19 nm)/Nb(10 nm)/Te(36 nm)/cordierite;

Sequence 3: Te(36 nm)/Nb(10 nm)/V(19 nm)/Mo(72 nm)/cordierite.

The XPS compositions in relative molar ratios of the as-deposited films on cordierite are shown in Table 4. Note that the ratios of the catalyst metals to Si, Al, Mg, and Na (constituents of cordierite) are not shown.

It can be seen that the deposition sequence affects the surface composition of the system. A key difference between the surface compositions of the films deposited on cordierite versus those deposited on Si wafer is that on the Mo-terminated surface on cordierite, there is evidence of V,

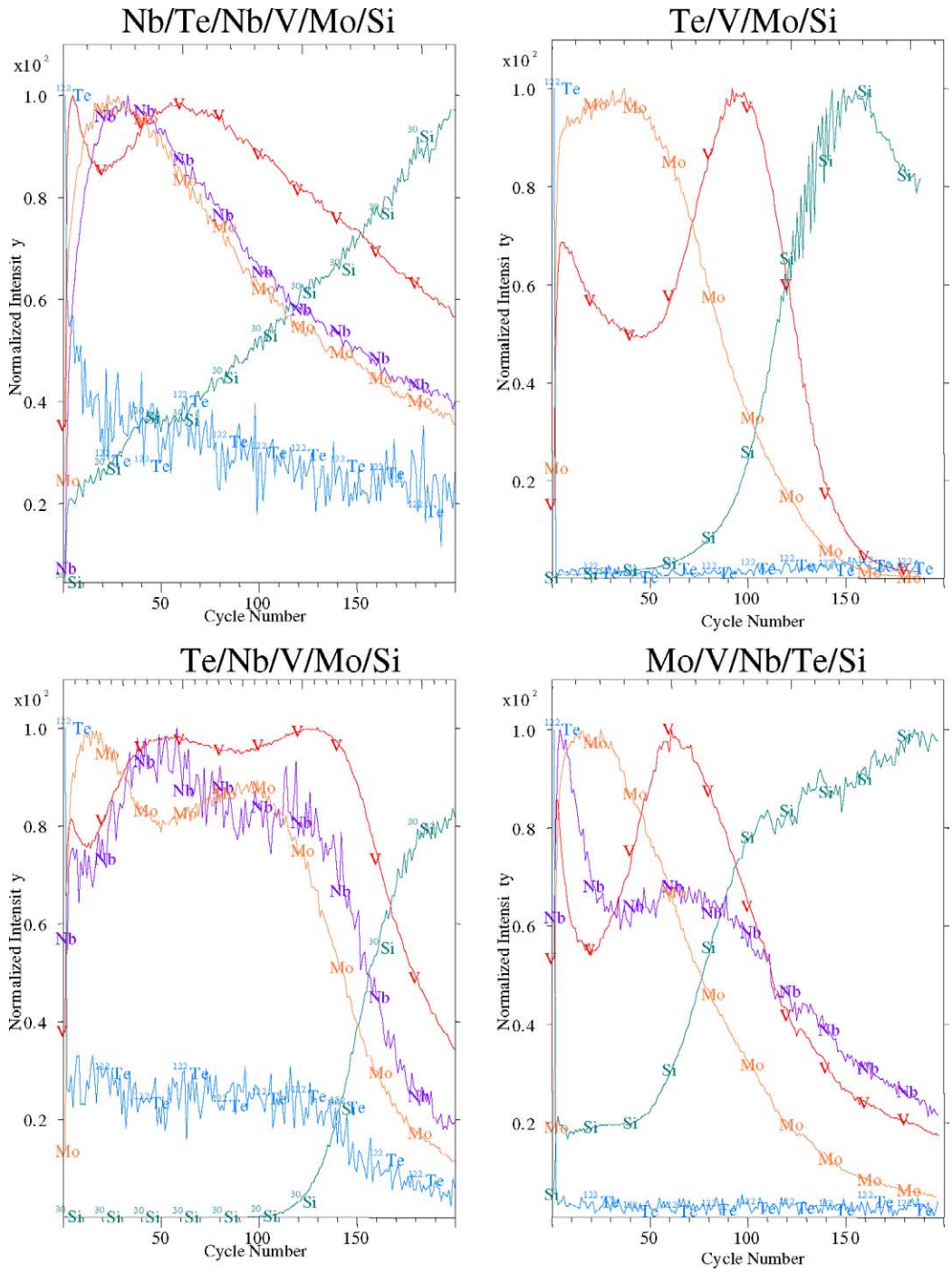

Fig. 8. SIMS profiles after calcination of PVD films for 2 h at 600 °C in air.

Table 4
XPS composition in relative molar ratios of as-deposited films on cordierite

Element	Te/Nb/V/Mo/cordierite		Mo/V/Nb/Te/cordierite	
	As deposited	SD	As deposited	SD
O	38.12	3.97	9.49	0.06
V	0.28	0.09	0.05	0.01
Mo	1.00	0.00	1.00	0.00
Nb	0.00	0.00	0.03	0.00
Te	4.04	0.42	0.13	0.01

Nb, and Te from the underlying layers. This may be due to the roughness of the cordierite surface compared to the smooth Si wafer where the Mo-terminated deposition sequence showed no evidence of any other metal (see Table 1).

These films were calcined at 275 °C in air followed by calcinations in a N_2 atmosphere at 600 °C. The progress of the catalysis was followed by an on-line gas chromatographic method that was set up to sample the effluent stream on-line for fixed gases, light hydrocarbons, and light or-

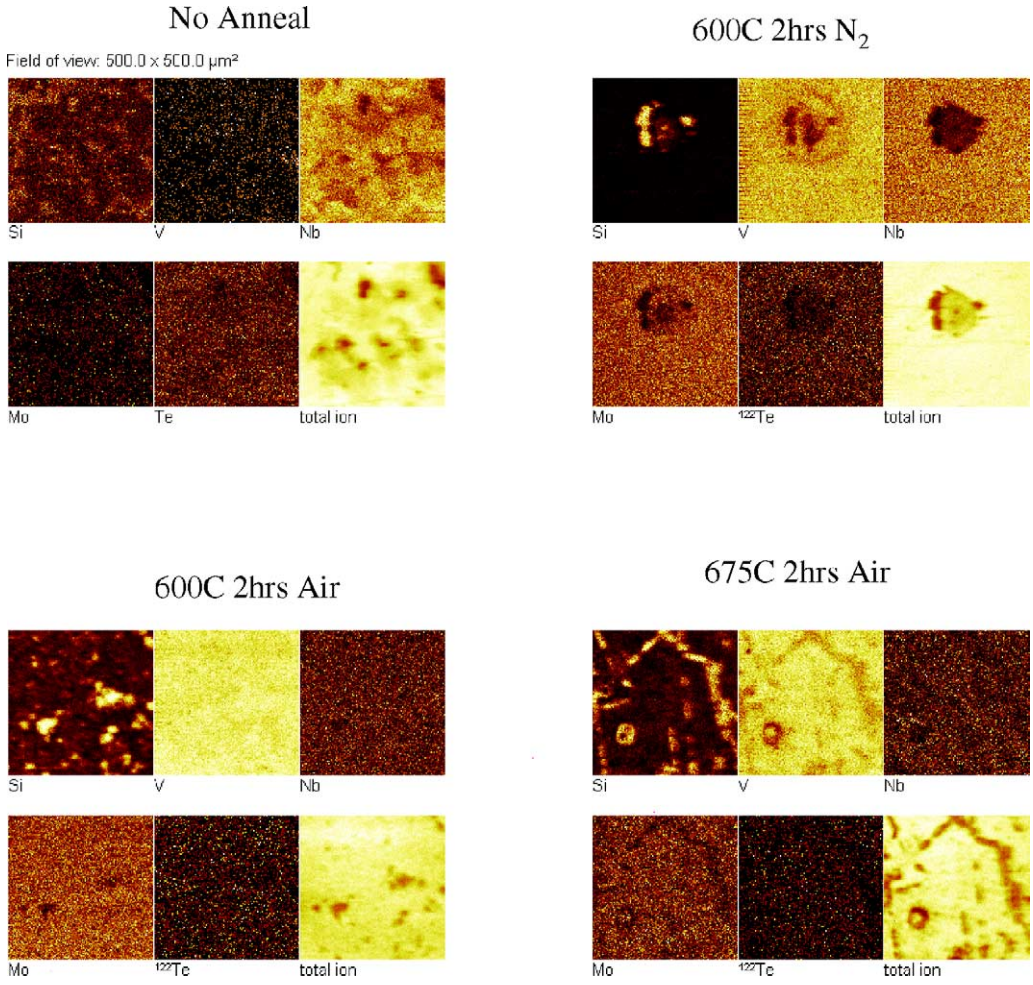

Fig. 9. SIMS images at the air interface after calcination treatment of Nb/Te/Nb/V/Mo/Si films under different conditions.

ganic acids. Samples were analyzed on a SRI 8610C gas chromatograph equipped with heated sampling valves, flame ionization detector, and thermal conductivity detector. The reactor effluent sample was injected into two systems; one for organic acids and the other for fixed gases and light hydrocarbons.

Results from the fixed-bed evaluation studies, which gave consistent and reproducible results with mass balances all in the range of 98 to 102%, are listed below.

Sample	Catalyst temp. (°C)	Propane conversion (%)	AA yield (%)	Propylene yield (%)
Sequence 1	480	32	21	3
Sequence 3	560	26	19	4

As a comparison, control calcinations studies were conducted on films deposited according to sequences 1 and 3. A set of samples were calcined in air up to 600 °C and evaluated under the run conditions given above. No activity was observed up to catalyst bed temperatures approaching 600 °C.

Shown in Table 5 are the XPS compositions in relative molar ratios of the catalysts calcined under various conditions. It can be seen that calcining the films at 275 °C in air followed by 600 °C in N_2 produces systems with similar surface compositions regardless of the deposition sequence. Note that both these systems showed activity toward formation of acrylic acid. This may be attributed to the presence of all four elements (Mo, V, Nb, and Te) on the surface. Comparison of the XPS data for both deposition sequences may lead one to the erroneous conclusion that calcining in air at 275 °C followed by N_2 at 600 °C should result in the same materials. But this is not the case from the reactor studies. Following this calcination procedure the Mo/V/Nb/Te/cordierite sample results in a catalyst that is significantly more active than that produced from the reverse deposition sequence. We were unable to obtain XRD patterns from the two catalysts since the amount of catalyst was not sufficient to yield a good signal. XRD patterns for both catalysts were similar and correspond to cordierite. We speculate that even though the XPS compositions are similar, the materials are different in terms of phases or structures, which may account for the different activities. Different phases with varying activity have been reported earlier for MoVNbTe oxides [26–31].

It is worth noting that even after the same calcination procedure (275 °C in air followed by 600 °C in N_2), the XPS

Table 5
XPS composition in relative molar ratios of calcined catalysts

	Te/Nb/V/Mo/cordierite		Mo/V/Nb/Te/cordierite		Te/Nb/V/Mo/cordierite		Stnd MMO catalyst	
Element	275 °C air, 600 °C N_2	SD	275 °C air, 600 °C N_2	SD	275 °C air, 600 °C air	SD	275 °C air, 600 °C N_2	SD
O	30.92	4.91	33.75	0.18	50.92	5.44	4.07	0.04
V	0.17	0.06	0.13	0.06	0.48	0.28	0.15	0.01
Mo	1.00	0.00	1.00	0.00	1.00	0.00	1.00	0.00
Nb	0.05	0.01	0.08	0.02	0.00	0.00	0.16	0.02
Te	0.50	0.06	0.44	0.08	1.51	0.61	0.39	0.01

composition for the film deposited on cordierite is quite different than that deposited on Si wafers (see Table 3). This is presumably due to two reasons. The first is that the cordierite surface is much rougher compared to the Si wafer. The second reason is that, when calcining in a N_2 atmosphere, there is no oxygen available for the Si wafer system, whereas for cordierite, there is plenty of oxygen available in bulk cordierite. This may change the diffusion characteristics of the various metals. In general, one can say that calcination in N_2 results in a Nb-rich surface for both systems.

The catalyst calcined in air showed no activity, presumably due to the absence of Nb on the surface. The XPS results revealed the absence of all four elements together on the surface. Also shown for reference is the XPS composition for a typical mixed metal oxide catalyst prepared by rotavaping the metal precursors (in the appropriate ratio) to prepare a bulk catalyst. When calcined in air at 275 °C followed by calcination in N_2 at 600 °C, this catalyst typically gives an excess of 40% AA yield. While the volumetric contact time in this case is 3–6 s, it is interesting to note the similarities in the XPS composition of this bulk catalyst compared to the thin film catalysts deposited on cordierite and calcined under similar conditions.

4. Conclusions

Based on the results and discussion presented above, the following conclusions can be made regarding the synthesis, characterization, and reactor evaluations under the experimental conditions described in the current paper:

1. The surface compositions of the calcined samples depend on the deposition sequence on Si wafers.
2. Calcination at 600 °C results in a diffusion of individual metal layers.
3. Compared to calcinations in N_2, calcination in air leads to a surface enrichment of V and Mo oxides and a reduction of Nb oxides.
4. Calcinations in N_2 is desirable for the formation of reduced Mo species.
5. Catalytic activity is related to the presence of all four metals (Mo, V, Nb, and Te) on the surface. Both deposition sequences on cordierite, after being calcined in air at 275 °C followed by calcination in N_2 at 600 °C, show good catalytic activity and they both have Nb on the surface.
6. Deposition sequence of Mo/V/Nb/Te/cordierite results in a catalyst that is significantly more active, with an AA yield up to 21%, than that produced from the reverse deposition sequence (Te/Nb/V/Mo/cordierite).

Acknowledgments

We acknowledge Rohm and Hass for financial support. We also acknowledge Exxon Mobil for providing beamtime for NEXAFS measurements.

References

[1] R.K. Grasselli, Catal. Today 49 (1999) 141.
[2] M. Baerns, O. Buyevskaya, Catal. Today 45 (1998) 13.
[3] G. Centi, S. Perathoner, F. Trifiro, Appl. Catal. A 157 (1997) 143.
[4] I. Matsuura, Shokubai (Japanese) 39 (1997) 39.
[5] X. Yang, Shiyou Huagong (Chinese) 24 (1995) 133.
[6] Y. Moro-Oka, W. Ueda, Catalysis 11 (1994) 223.
[7] A.T. Guttmann, R.K. Grasselli, J.F. Brazdil, D.D. Suresh, US Patent 4,746,641 (1988).
[8] M. Hatano, A. Kayo, US Patent 5,049,692 (1991).
[9] M.M. Lin, Appl. Catal. A 207 (2001) 1.
[10] E. Thorsteinson, T. Wilson, F. Young, P. Kasai, J. Catal. 52 (1978) 116.
[11] J. Bartek, A. Ebner, J. Brazdil, US Patent 5,198,580 (1993).
[12] G. Blanchard, G. Ferre, EP Patent 609,122-A1 (1994).
[13] C. Mazzocchia, E. Tempesti, R. Anouchinsky, A. Kaddouri, FR Patent 2,693,384 (1994).
[14] T. Ushikubo, H. Nakamura, Y. Koyasu, S. Wajiki, US Patent 5,380,933 (1995).
[15] T. Ushikubo, Y. Koyasu, H. Nakamura, S. Wajiki, JP Patent 98,045,664 (1998).
[16] M. Takahashi, S. To, S. Hirose, JP Patent 98,118,491 (1998).
[17] M. Takahashi, S. To, S. Hirose, JP Patent 98,120,617 (1998).
[18] M. Lin, M. Linsen, US Patent 6,180,825 (2001); US Patent 6,514,901 (2003); US Patent 6,514,903 (2003).
[19] L. Luo, J. Labinger, M. Davis, in: Catalysis and Surface Science, Poster, 219th ACS Meeting, March 2000.
[20] M. Hatano, A. Kayo, EP Patent 0,318,295 B1 (1992).
[21] M. Lin, C. Long, M. Linsen, F. Kaiser, P. Klugherz, J. McGregor, M. Clark, in: Catalysis and Surface Science, Symposium, 219th ACS Meeting, March 2000.
[22] H. Watanabe, Y. Koyasu, Appl. Catal. A 194–195 (2000) 479.
[23] J.G. Chen, Surf. Sci. Rep. 30 (1997) 1.
[24] C.M. Kim, B.D. DeVries, B. Fruhberger, J.G. Chen, Surf. Sci. 327 (1995) 81.
[25] J.G. Chen, B. Fruhberger, M.L. Colaianni, J. Vac. Sci. Technol. A 14 (1996) 1668.
[26] R.K. Grasselli, J.D. Burrington, D.J. Buttrey, P. DeSanto Jr., C.G. Lugmair, A.F. Volpe Jr., T. Weingand, Top. Catal. 23 (2003) 5.
[27] P. DeSanto Jr., D.J. Buttrey, R.K. Grasselli, C.G. Lugmair, A.F. Volpe, B.H. Toby, T. Vogt, Top. Catal. 23 (2003) 23.
[28] M. Aouine, J.L. Duboise, J.M.M. Millet, Chem. Commun. 13 (2001) 1180.
[29] E. Garcia-Gonzalez, J.M. Nieto, P. Botella, J.M. Gonzalez-Calbet, Chem. Mater. 14 (2002) 4416.
[30] J. Holmberg, R.K. Grasselli, A. Andersson, Top. Catal. 23 (2003) 55.
[31] M. Baca, A. Pigamo, J.L. Dubois, J.M.M. Millet, Top. Catal. 39 (2003) 39.